Demonstrator Notes for the green line experiment.

Appendix A1. Understanding the Hyperfine structure of Mercury

Energy Levels of Mercury (the Grotrian diagram).

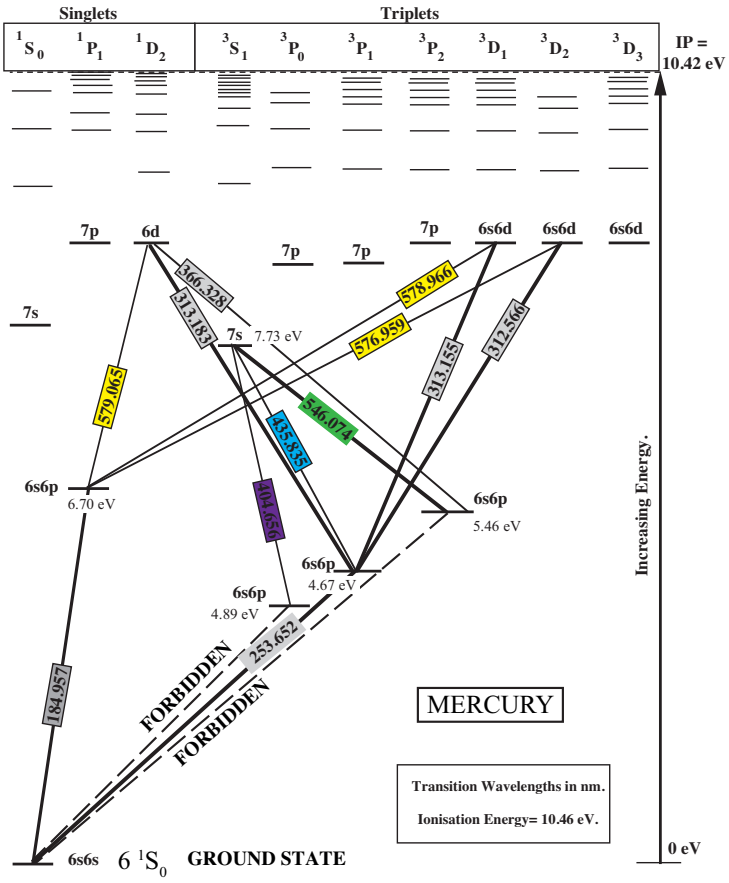

FIG A1. Grotrian diagram of Hg showing the different states and their relative energies. The wavelengths of several allowed optical transitions are also shown. The 546.047 nm line is the transition that is studied in this experiment. The strongest lines are the UV transitions at ~185 nm and ~254 nm. Transitions from the 6^3P_2 and 6^3P_0 states are forbidden from dipole selection rules, so these states are *metastable*. The transition from the 6^3P_1 state *is* allowed since the states in Hg are more accurately defined as a mixture of singlet and triplet states. For strict LS coupling (as in helium) transitions from triplet to singlet states are not allowed (look up the Grotrian diagram from He to see this) and so in this atom the lowest 2^3S_1 state cannot decay back to the 2^1S_0 ground state.

Figure A1 shows the energy level diagram of mercury (represented as a *Grotrian diagram*). The states are divided into singlet states and triplet states, which represent the total spin of the electrons. Mercury has 80 electrons, with 78 of them in the closed n=1 to n=5 orbitals (or 'shells'). The integer n is called the ***Principal Quantum Number***. The outer two valence electrons are in the n=6 orbital, so that mercury has a similar energy level structure to helium (which only has two electrons). The atom is represented here in *LS* coupling, where the spin and orbital angular momenta are considered to occupy different (Hilbert) spaces. You should look up the Grotrian diagram of helium to see the similarities and differences between the two atoms.

The ground state of mercury is the 6^1S_0 state as shown, with both outer electrons being 6s electrons (often written as $6s^2$). The full representation of all electrons in Hg in the ground state is then given by (you should look up why):

$$\left(\underbrace{1s^2 2s^2 2p^6 3s^2 3p^6 3d^{10} 4s^2 4p^6 4d^{10} 4f^{14} 5s^2 5p^6 5d^{10}}_{78\,\text{electrons in inner 'shells'}} \right) 6s^2\ {}^1S_0 .$$

It is usual to only consider the outer electrons since the inner electrons usually do not play a role in the excitation process (to a first approximation – we do not know which electrons are promoted, only that when we make a measurement of an excited atom as in figure 1 that one of them has been).
Only one of the electrons is excited to produce the various measured neutral states of the atom as shown. The ionization energy (IP) is 10.42 eV, after which one of the electrons will be released, leaving a mercury ion Hg^+. The excited states we are considering here are those shown coupled by radiation at 546nm.

Representation of the atom in *LS* coupling.

In *LS* coupling (also known as Russell-Saunders coupling) it is assumed that the spin of the individual electrons $\boldsymbol{s}_i$ (i=1 to 80 for Hg) all couple together independently of their orbital angular momenta $\boldsymbol{l}_i$, with any final interaction occurring between the total spin of the electrons **S** and the total orbital angular momentum **L**. The other extreme is called *jj-coupling*, where each individual electron spin $\boldsymbol{s}_i$ couples to its own orbital angular momentum $\boldsymbol{l}_i$ to form a sum $\boldsymbol{j}_i$, the total angular momentum then being the sum of the $\boldsymbol{j}_i$. There are other *intermediate coupling schemes* possible between these extremes. If you do the Franck Hertz experiment in this lab you will come across one of these that represents neon.

In *LS* coupling the total spin of all electrons in the atom is represented as the superscript on the left hand side of the state. This is given by $2S_{tot}+1$, where S_{tot} is the magnitude of the total spin of all of the electrons in the atom each with a spin $\boldsymbol{s_i}$, so that $S_{tot}=\sum_{i=1}^{80} s_i$. Hence for a singlet state $S_{tot}=0$ and for a triplet state $S_{tot}=1$. Each electron has a spin of ½ (in units of $\hbar$), and to minimise the energy of the atom the 78 inner shell electrons pair up with opposite spins (so the total spin of all inner electrons is zero). In the lowest energy (the ground state), the outer 2 electrons also pair with opposite spins so that again their total spin is zero. The total spin of all electrons in the ground state atom is hence zero, so that $2S_{tot}+1=1$: this is a *singlet state*. For triplet states the outer 2 electrons have the same spin direction, so that their total spin is then S = ½ + ½ =1. In this case $2S_{tot}+1=3$. Electrons with the same spin tend to avoid each other as they orbit the nucleus, due to the Pauli Exclusion Principle. This has consequences for the energy of the states, as described below.

Again in LS coupling the orbital angular momenta of each individual electron is l_i and so the total orbital angular momentum of the 80 electrons is $L=\sum_{i=1}^{80} l_i$. This is represented by the symbol S (the *sharp* series), P (the *principal* series), D (the *diffuse* series) etc. These are historical names from spectroscopy, when the reasons for the different series that were observed was unknown. Again for the inner 78 electrons their individual orbital angular momenta l_i all add to give a total angular momentum of zero, since this produces the lowest energy. The outer 2 electrons can have different individual orbital angular momenta ranging from $l_i=l_{79,80}=0\ldots\infty$ with $0<l_i<n-1$. Since the energy of the states is below the IP only one of the electrons in the excited state carries angular momentum, the other remaining in an s-state with $l_i=0$ (this is a 6s electron as shown). The individual electron orbital angular momenta are represented by the symbols s, p, d etc. and so the excited states can be an S-state ($l_{79}=l_{80}=0$), a P-state ($l_{79}=0;l_{80}=1\,\text{or}\,l_{79}=1;l_{80}=0$), a D-state ($l_{79}=0;l_{80}=2\,\text{or}\,l_{79}=2;l_{80}=0$) etc.

It is possible to produce atoms with both electrons excited (a *doubly excited* state) however the total energy of the atom is then greater than the IP and so the atom will quickly ionize. These states *can* be detected using sophisticated experiments, however they are not important for the discussion here.

In LS coupling the total angular momentum of the atom $\boldsymbol{J}$ due to the electrons is given by the vectorial summation of the total spin of the electrons $\boldsymbol{S}$ and the total orbital angular momentum $\boldsymbol{L}$, so that $\boldsymbol{J} = \boldsymbol{L} + \boldsymbol{S}$. As with all quantum mechanics the magnitude of the angular momentum $\boldsymbol{J}$ is quantized when measured, so that the magnitude of $\boldsymbol{J}$ ranges from $J = L+S, L+S-1, \ldots, |L-S|$. The value of J is represented as the lower subscript on the right hand side of the state symbol. The ground 6^1S_0 state of Hg is hence represented by the quantum numbers $n=6, L=0(S-state), S=0(2S_{tot}+1=0), J=0$ whereas the excited 6^3P_2 state is represented by the quantum numbers $n=6, L=1, S=1, J=2$.

The first excited states of mercury occur when one of the electrons is excited to be a 6p electron, with angular momentum $l=1$. Under these conditions, four 6P states are possible. These are given by:

$$\left.\begin{array}{l} n=6, L=1, S=0, J=1:\ 6^1P_1 \end{array}\right\} \text{Singlet state}$$

$$\left.\begin{array}{l} n=6, L=1, S=1, J=2:\ 6^3P_2 \\ n=6, L=1, S=1, J=1:\ 6^3P_1 \\ n=6, L=1, S=1, J=0:\ 6^3P_0 \end{array}\right\} \text{Triplet states}$$

Since the total angular momentum of the triplet states varies from $J = 2$ to $J = 0$, this creates a relative change in energy of the excited states. This difference in energy due to the total angular momentum J is called the ***Fine Structure Splitting***. The fine structure splitting is the mechanism that produces the familiar doublet lines in sodium.

In helium the difference in energy of the triplet states due to the fine structure splitting is very small (<1 meV) and so is difficult to resolve unless lasers are used. By contrast, in mercury this difference is more than 800 times larger than in helium, as seen in figure A1. This is a consequence of the complex nature of the atom and means that the fine structure splitting for the 6P states is easy to resolve.

The difference in energy between singlet and triplet states arises due to the Pauli exclusion principal as noted above. Electrons in states with the same spin quantum numbers tend to avoid each other (i.e. triplet state electrons), so their mutual Coulomb repulsion has a reduced energy compared to electrons in different spin states (the singlet states) that can approach each other more closely (and hence feel a stronger repulsion). Triplet states are hence usually lower in energy than their corresponding singlet states, as seen in figure A1. *This difference is purely a quantum mechanical effect and has no analogy in classical physics.*

The transition that is studied in this experiment is the $7^3S_1 \rightarrow 6^3P_2$ decay at ~546 nm. This is a convenient transition as it can easily be resolved from other transitions as shown, by using a narrow bandwidth interference filter to select only this radiation. The states used in this experiment are hence represented by the following quantum numbers:

$$\left.\begin{array}{l} n=7, L=0, S=1, J=1:\ 7^3S_1 \end{array}\right\} \text{Upper state}$$

$$\left.\begin{array}{l} n=6, L=2, S=1, J=2:\ 6^3P_2 \end{array}\right\} \text{Lower states}$$

Effect of the nuclear spin on the energy levels.

As noted above, neutral mercury has 80 electrons and so also has 80 protons within the nucleus. To stabilize the nucleus from disintegration due to Coulomb repulsion between protons, it is necessary to include neutrons within the nucleus. Naturally occurring mercury has seven stable *isotopes*, with different numbers of neutrons N_n. These are the ^{196}Hg,^{198}Hg,^{199}Hg,^{200}Hg,^{201}Hg,^{202}Hg and ^{204}Hg isotopes. Since protons and neutrons have a nuclear spin of ½, the spins of the 80 protons sum to zero (the lowest energy state). For the even isotopes the nuclear spins of the neutrons i_μ also pair up to sum to zero, so that their total nuclear spin $I = \sum_{\mu=1}^{N_n} i_\mu$ is zero. For the two odd isotopes in Hg there is an unpaired neutron and so each of these isotopes must have a non-zero nuclear spin. For the ^{199}Hg isotope the nuclear spin is I = ½. For the ^{201}Hg isotope the total nuclear spin is I=3/2.

In the same way as for the fine structure splitting, the total angular momentum $\boldsymbol{F}$ of the atom depends on the nuclear spin $\boldsymbol{I}$ and how this vectorially adds to the total angular momentum of the electrons $\boldsymbol{J}$. Hence $\boldsymbol{F} = \boldsymbol{J} + \boldsymbol{I}$ with the magnitude of **F** ranging from $F = J + I, J + I - 1, \ldots, |J - I|$.

The energy splitting that occurs due to differences in the value of *F* is called the ***Hyperfine Structure Splitting***. This is much smaller that the fine structure splitting and so can only be resolved using a very high-resolution spectrometer, or laser system. In the experiments you are working on here, a high-resolution Fabry-Perot interferometer is used to detect these differences in energy, through observing the 546 nm transition.

As noted, for ^{199}Hg I = ½ and for ^{201}Hg I = 3/2. The upper excited state is the 7^3S_1 state and so the value of *F* ranges from $F = I + J$ to $|I - J|$. For the ^{199}Hg isotope the 7^3S_1 state splits into the F = 3/2 and F = ½ hyperfine states. For the ^{201}Hg isotope the 7^3S_1 state splits into the F = 5/2, 3/2 and ½ state.

The lower state is the 6^3P_2 state with L = 1, S = 1 and J = 2. For the ^{199}Hg isotope the 6^3P_2 state hence splits into the F = 5/2 and 3/2 hyperfine states. For the ^{201}Hg isotope the 6^3P_2 state splits into the F = 7/2, 5/2, 3/2 and ½ states, as is shown in figure A2.

The mass (isotope) shift.

A small change in energy of the isotopic states also occurs due to the different masses of the nuclei. This arises due to small physical changes in the nucleus as the number of nucleons is varied. For light atoms this effect is dominated by the relative change in the centre of mass of the atom, which changes the Coulomb interaction by a small amount. For heavy atoms such as mercury, the energy shift is dominated by a restructure of the nuclear shape to accommodate the different number of neutrons. This leads to a small deformation of the nucleus, with a subsequent change in the total Coulomb interaction between the protons and the orbiting electrons (the nucleus can no longer be considered as a 'point source' under these conditions, and so the interaction depends on the position of each of the protons distributed throughout the deformed nucleus). The change in energy due to this effect is difficult to calculate theoretically and so is usually measured experimentally, using very high-resolution lasers. Since these energy differences are smaller than can be resolved using the Fabry Perot spectrometer in this experiment, the mass shifts for the different isotopes of mercury are given here, as taken from the laser measurements of Sansonetti et al.

Calculation of the Hyperfine Structure Splitting.

Although the mass shift is too small to measure in these experiments, the energy shift due to the hyperfine interaction is much larger and so can be resolved. It can be shown that the interaction Hamiltonian for the hyperfine state energy splittings is given by [see Bransden & Joachain]:

$$H^{HFS} = a^{HF}\left(\mathbf{I}\cdot\mathbf{J}/\hbar^2\right) + b^{HF}\left(\frac{3\left(\mathbf{I}\cdot\mathbf{J}/\hbar^2\right)^2 + 3\left(\mathbf{I}\cdot\mathbf{J}/2\hbar^2\right) - \left(\mathbf{I}^2\mathbf{J}^2/\hbar^4\right)}{2I\left(2I-1\right)J\left(2J-1\right)}\right) \qquad \text{(A1)}$$

where $\left(a^{HF}, b^{HF}\right)$ are the magnetic dipole & electric quadrupole constants respectively. For I= 0,1/2 and for J=0,1/2 the coefficient $b^{HF} = 0$ from symmetry ([see Corney]). Since we can write $\left(\mathbf{I}\cdot\mathbf{J}\right) = \frac{1}{2}\left(\mathbf{F}^2 - \mathbf{I}^2 - \mathbf{J}^2\right)$ and that $\mathbf{F}^2 = \mathbf{F}\cdot\mathbf{F} = F^2$ etc., the interaction Hamiltonian can then be rewritten as:

$$H^{HFS} = a^{HF}\left(\mathbf{I}\cdot\mathbf{J}/\hbar^2\right) + b^{HF}\left(\frac{3\left(\mathbf{I}\cdot\mathbf{J}/\hbar^2\right)^2 + 3\left(\mathbf{I}\cdot\mathbf{J}/2\hbar^2\right) - \left(\mathbf{I}^2\mathbf{J}^2/\hbar^4\right)}{2I\left(2I-1\right)J\left(2J-1\right)}\right)$$

$$\therefore H^{HFS} = \left(\begin{array}{l} \dfrac{a^{HF}}{2\hbar^2}\left(F^2 - I^2 - J^2\right) \\ + \dfrac{b^{HF}}{2I\left(2I-1\right)J\left(2J-1\right)}\left(3\left(\dfrac{F^2 - I^2 - J^2}{2\hbar^2}\right)^2 + \dfrac{3}{2}\left(\dfrac{F^2 - I^2 - J^2}{2\hbar^2}\right) - \dfrac{I^2J^2}{\hbar^4}\right) \end{array}\right) \qquad \text{(A2)}$$

First consider the magnetic component $H^{HFSa} = \frac{a^{HF}}{2\hbar^2}\left(F^2 - I^2 - J^2\right)$. If the eigenstates of the system are represented by $\left|F,I,J\right\rangle$ which are all good quantum numbers, then in atomic units in this representation we have [see Bransden & Joachain]:

$$\left.\begin{array}{l} F^2\left|F,I,J\right\rangle = F\left(F+1\right)\hbar^2\left|F,I,J\right\rangle \\ I^2\left|F,I,J\right\rangle = I\left(I+1\right)\hbar^2\left|F,I,J\right\rangle \\ J^2\left|F,I,J\right\rangle = J\left(J+1\right)\hbar^2\left|F,I,J\right\rangle \end{array}\right\} \qquad \text{(A3)}$$

The interaction energy can then be written using first order perturbation theory as:

$$\Delta E^{HFSa} = \left\langle F',I',J'\right|H^{HFSa}\left|F,I,J\right\rangle = \frac{a^{HF}}{2\hbar^2}\left(F\left(F+1\right) - I\left(I+1\right) - J\left(J+1\right)\right)\hbar^2 = \frac{a^{HF}K}{2} \qquad \text{(A4)}$$

where $K = F\left(F+1\right) - I\left(I+1\right) - J\left(J+1\right)$. Since the ^{199}Hg isotope has no quadrupole moment we have:

$^{199}Hg\,7^3S_1\left(I=1/2\right)$:

$$\Delta E^{HFSa}=\frac{a_{S^{199}}^{HF}}{2\hbar^2}\left(F\left(F+1\right)-I\left(I+1\right)-J\left(J+1\right)\right)\hbar^2$$

$$\Delta E^{HFSa}=\frac{a_{S^{199}}^{HF}}{2}\left(F\left(F+1\right)-\frac{1}{2}\left(\frac{1}{2}+1\right)-1\left(1+1\right)\right)=\frac{a_{S^{199}}^{HF}}{2}\left(F\left(F+1\right)-\frac{11}{4}\right)$$

$$\therefore \Delta E_{F=3/2}^{HFSa}=\frac{a_{S^{199}}^{HF}}{2}\left(\frac{3}{2}\left(\frac{3}{2}+1\right)-\frac{11}{4}\right)=+\frac{1}{2}a_{S^{199}}^{HF};\ \Delta E_{F=1/2}^{HFSa}=\frac{a_{S^{199}}^{HF}}{2}\left(\frac{1}{2}\left(\frac{1}{2}+1\right)-\frac{11}{4}\right)=-a_{S^{199}}^{HF}\qquad\text{(A5)}$$

$$\therefore \Delta E_{F=3/2}^{HFSa}-\Delta E_{F=1/2}^{HFSa}=+\frac{1}{2}a_{S^{199}}^{HF}+a_{S^{199}}^{HF}=\frac{3}{2}a_{S^{199}}^{HF}=32{,}250\text{ MHz}$$

$$\Rightarrow a_{S^{199}}^{HF}=21{,}500\text{ MHz}$$

$$\therefore \Delta E_{F=3/2}^{HFSa}=+\frac{1}{2}a_{S^{199}}^{HF}=+10{,}750\text{ MHz};\quad \Delta E_{F=1/2}^{HFSa}=-a_{S^{199}}^{HF}=-21{,}500\text{ MHz}$$

where the energy is written in MHz for convenience and the state splitting is taken from [laser paper].

We also have:

$^{199}Hg\,6^3P_2\left(I=1/2\right)$:

$$\therefore \Delta E^{HFSa}=\frac{a_{P^{199}}^{HF}}{2\hbar^2}\left(F\left(F+1\right)-I\left(I+1\right)-J\left(J+1\right)\right)\hbar^2$$

$$\Delta E^{HFSa}=\frac{a_{P^{199}}^{HF}}{2}\left(F\left(F+1\right)-\frac{1}{2}\left(\frac{1}{2}+1\right)-2\left(2+1\right)\right)=\frac{a_{P^{199}}^{HF}}{2}\left(F\left(F+1\right)-\frac{27}{4}\right)$$

$$\therefore \Delta E_{F=5/2}^{HFSa}=\frac{a_{P^{199}}^{HF}}{2}\left(\frac{5}{2}\left(\frac{5}{2}+1\right)-\frac{27}{4}\right)=+a_{P^{199}}^{HF};\Delta E_{F=3/2}^{HFSa}=\frac{a_{P^{199}}^{HF}}{2}\left(\frac{3}{2}\left(\frac{3}{2}+1\right)-\frac{27}{4}\right)=-\frac{3}{2}a_{P^{199}}^{HF}\qquad\text{(A6)}$$

$$\therefore \Delta E_{F=5/2}^{HFSa}-\Delta E_{F=3/2}^{HFSa}=+a_{P^{199}}^{HF}+\frac{3}{2}a_{P^{199}}^{HF}=\frac{5}{2}a_{S^{199}}^{HF}=22{,}666\text{ MHz}$$

$$\Rightarrow a_{P^{199}}^{HF}=9{,}066.4\text{ MHz}$$

$$\therefore \Delta E_{F=5/2}^{HFSa}=+a_{P^{199}}^{HF}=9{,}066.4\text{ MHz};\quad \Delta E_{F=3/2}^{HFSa}=-\frac{3}{2}a_{P^{199}}^{HF}=-13{,}599.6\text{ MHz}$$

The ^{201}Hg does have a quadrupole moment. This adds an amount given by the Hamiltonian:

$$H^{HFSQ}\left|F,I,J\right\rangle = b^{HF}\left(\frac{3\left(\frac{\mathbf{I}\cdot\mathbf{J}}{\hbar^2}\right)^2+3\left(\frac{\mathbf{I}\cdot\mathbf{J}}{2\hbar^2}\right)-\frac{\mathbf{I}^2\mathbf{J}^2}{\hbar^4}}{2I\left(2I-1\right)J\left(2J-1\right)}\right)\left|F,I,J\right\rangle$$

$$= b^{HF}\left(\frac{3\left(\frac{K\hbar^2}{2\hbar^2}\right)^2+3\left(\frac{K\hbar^2}{2\hbar^2}\right)\Big/2-\frac{I^2J^2\hbar^4}{\hbar^4}}{2I\left(2I-1\right)J\left(2J-1\right)}\right)\left|F,I,J\right\rangle = b^{HF}\left(\frac{3\frac{K^2}{4}+3\left(\frac{K}{4}\right)-I\left(I-1\right)J\left(J-1\right)}{2I\left(2I-1\right)J\left(2J-1\right)}\right)\left|F,I,J\right\rangle \qquad \text{(A7)}$$

$$= b^{HF}\left(\frac{3K^2+3K-4I\left(I-1\right)J\left(J-1\right)}{8I\left(2I-1\right)J\left(2J-1\right)}\right)\left|F,I,J\right\rangle$$

The hyperfine energy shift including the quadrupole interaction term for the 7^3S_1 state is hence given by:

$$\Delta E^{HF}_{S^{201}} = \frac{a^{HF}_{S^{201}}K}{2}+\frac{b^{HF}_{S^{201}}}{8}\left(\frac{3K\left(K+1\right)-4I\left(I+1\right)J\left(J+1\right)}{I\left(2I-1\right)J\left(2J-1\right)}\right) \qquad \text{(A8)}$$

For this state we have:

$$K = \left(F\left(F+1\right)-J\left(J+1\right)-I\left(I+1\right)\right)=\left(F\left(F+1\right)-\frac{23}{4}\right)$$

$$\Rightarrow K^{F=1/2}=-5; K^{F=3/2}=-2; K^{F=5/2}=+3$$

This then gives the following hyperfine state splittings:

$$\left.\begin{aligned}
\Delta E^{HF}_{F=1/2} &= \frac{a^{HF}_{S^{201}}\left(K\right)}{2}+\frac{b^{HF}_{S^{201}}}{8}\left(\frac{3\left(K\right)\left(K+1\right)-4I\left(I+1\right)J\left(J+1\right)}{I\left(2I-1\right)J\left(2J-1\right)}\right)=\frac{\left(K\right)}{2}a^{HF}_{S^{201}}+\left(\frac{\left(K\right)\left(K+1\right)-10}{8}\right)b^{HF}_{S^{201}}\\
\Delta E^{HF}_{F=1/2} &= \frac{a^{HF}_{S^{201}}\left(-5\right)}{2}+\left(\frac{\left(-5\right)\left(-5+1\right)-10}{8}\right)b^{HF}_{S^{201}}=-\frac{5}{2}a^{HF}_{S^{201}}+\frac{5}{4}b^{HF}_{S^{201}}\\
\Delta E^{HF}_{F=3/2} &= \frac{a^{HF}_{S^{201}}\left(-2\right)}{2}+\left(\frac{\left(-2\right)\left(-2+1\right)-10}{8}\right)b^{HF}_{S^{201}}=-a^{HF}_{S^{201}}-b^{HF}_{S^{201}}\\
\Delta E^{HF}_{F=5/2} &= \frac{a^{HF}_{S^{201}}\left(3\right)}{2}+\left(\frac{\left(3\right)\left(3+1\right)-10}{8}\right)b^{HF}_{S^{201}}=\frac{3}{2}a^{HF}_{S^{201}}+\frac{1}{4}b^{HF}_{S^{201}}
\end{aligned}\right\} \qquad (9)$$

The splittings between the states are hence:

$$\left|\Delta E^{HF}_{F=1/2}-\Delta E^{HF}_{F=3/2}\right|=11{,}926\ MHz=\left(-\frac{5}{2}a^{HF}_{S^{201}}+\frac{5}{4}b^{HF}_{S^{201}}\right)+\left(a^{HF}_{S^{201}}+b^{HF}_{S^{201}}\right)=\left(-\frac{3}{2}a^{HF}_{S^{201}}+\frac{9}{4}b^{HF}_{S^{201}}\right)$$

$$\left|\Delta E^{HF}_{F=3/2}-\Delta E^{HF}_{F=5/2}\right|=19{,}867\ MHz=\left(-a^{HF}_{S^{201}}-b^{HF}_{S^{201}}\right)-\left(\frac{3}{2}a^{HF}_{S^{201}}+\frac{1}{4}b^{HF}_{S^{201}}\right)=\left(-\frac{5}{2}a^{HF}_{S^{201}}-\frac{5}{4}b^{HF}_{S^{201}}\right)$$

$$\left|\Delta E^{HF}_{F=1/2}-\Delta E^{HF}_{F=5/2}\right|=31{,}793\ MHz=\left(-\frac{5}{2}a^{HF}_{S^{201}}+\frac{5}{4}b^{HF}_{S^{201}}\right)-\left(\frac{3}{2}a^{HF}_{S^{201}}+\frac{1}{4}b^{HF}_{S^{201}}\right)=\left(-4a^{HF}_{S^{201}}+b^{HF}_{S^{201}}\right)\qquad\text{(A10)}$$

$$\therefore\left|-6a^{HF}_{S^{201}}+9b^{HF}_{S^{201}}\right|=47{,}704\ MHz$$

$$\left|-10a^{HF}_{S^{201}}-5b^{HF}_{S^{201}}\right|=79{,}468\ MHz$$

$$\left|-4a^{HF}_{S^{201}}+b^{HF}_{S^{201}}\right|=31{,}793\ MHz$$

The solution is then given by:

$$-60a^{HF}_{S^{201}}+90b^{HF}_{S^{201}}=\pm477{,}040\ MHz$$

$$60a^{HF}_{S^{201}}+30b^{HF}_{S^{201}}=\mp476{,}808\ MHz$$

$$\therefore 120b^{HF}_{S^{201}}=\pm477{,}040\mp476{,}808=\pm232,\pm953848$$

$$\therefore b^{HF}_{S^{201}}=\pm1.933,\pm7{,}948.733\ MHz$$

$$-30a^{HF}_{S^{201}}+45b^{HF}_{S^{201}}=\pm238{,}520\ MHz$$

$$-90a^{HF}_{S^{201}}-45b^{HF}_{S^{201}}=\pm715{,}212\ MHz$$

$$\therefore -120a^{HF}_{S^{201}}=\pm238{,}520+\pm715{,}212$$

$$\therefore a^{HF}_{S^{201}}=\mp7{,}947.767\ MHz\qquad\text{(A11)}$$

$$-4a^{HF}_{S^{201}}+b^{HF}_{S^{201}}=-4\left(\mp7{,}947.767\right)+\left(\pm1.933\right)=\pm31791.067\pm1.933=\pm31{,}793$$

$$or-4a^{HF}_{S^{201}}+b^{HF}_{S^{201}}=-4\left(\mp7{,}947.767\right)+\left(\pm7{,}948.733\right)=\pm31791.067\pm7{,}948.733=\pm39{,}739.8$$

$$\left\langle a^{HF}_{S^{201}}\right\rangle=\mp7{,}946.71\ MHz;\left\langle b^{HF}_{S^{201}}\right\rangle=\pm4.79\ MHz$$

$$\left.\begin{aligned}\therefore\Delta E^{HF}_{F=1/2}&=-\frac{5}{2}a^{HF}_{S^{201}}+\frac{5}{4}b^{HF}_{S^{201}}=+19{,}873\ MHz\\ \Delta E^{HF}_{F=3/2}&=-a^{HF}_{S^{201}}-b^{HF}_{S^{201}}=+7{,}942\ MHz\\ \Delta E^{HF}_{F=5/2}&=\frac{3}{2}a^{HF}_{S^{201}}+\frac{1}{4}b^{HF}_{S^{201}}=-11{,}921\ MHz\end{aligned}\right\}$$

From experiments the ½ state is higher in energy, and so the solution is:

$$\left\langle a^{HF}_{S^{201}}\right\rangle=-7{,}946.71\ MHz;\left\langle b^{HF}_{S^{201}}\right\rangle=+4.79\ MHz\ .$$

The hyperfine energy shift including the quadrupole interaction term for the 6^3P_2 state is given by:

$$\Delta E^{HF}_{S^{201}}=\frac{a^{HF}_{P^{201}}K}{2}+\frac{b^{HF}_{P^{201}}}{8}\left(\frac{3K\left(K+1\right)-4I\left(I+1\right)J\left(J+1\right)}{I\left(2I-1\right)J\left(2J-1\right)}\right)\qquad\text{(A12)}$$

We now have:

$$K=\left(F\left(F+1\right)-J\left(J+1\right)-I\left(I+1\right)\right)=\left(F\left(F+1\right)-\frac{39}{4}\right)\qquad\text{(A13)}$$

$$\Rightarrow K^{F=1/2}=-9;K^{F=3/2}=-6;K^{F=5/2}=-1;K^{F=7/2}=+6$$

This then gives the hyperfine state splittings as follows:

$$\Delta E^{HF}_{F=1/2} = \frac{a^{HF}_{P^{201}}(K)}{2} + \frac{1}{8}\left(\frac{3(K)(K+1) - 4I(I+1)J(J+1)}{I(2I-1)J(2J-1)}\right) b^{HF}_{P^{201}}$$

$$= \frac{1}{2} a^{HF}_{P^{201}}(K) + \left(\frac{(K)(K+1)-30}{48}\right) b^{HF}_{P^{201}} \qquad \text{(A14)}$$

$$\left.\begin{aligned}
\Delta E^{HF}_{F=1/2} &= \frac{a^{HF}_{P^{201}}(-9)}{2} + \left(\frac{(-9)(-9+1)-30}{48}\right) b^{HF}_{P^{201}} = -\frac{9}{2} a^{HF}_{P^{201}} + \frac{7}{8} b^{HF}_{P^{201}} \\
\Delta E^{HF}_{F=3/2} &= \frac{a^{HF}_{P^{201}}(-6)}{2} + \left(\frac{(-6)(-6+1)-30}{48}\right) b^{HF}_{P^{201}} = -3 a^{HF}_{P^{201}} \\
\Delta E^{HF}_{F=5/2} &= \frac{a^{HF}_{P^{201}}(-1)}{2} + \left(\frac{(-1)(-1+1)-30}{48}\right) b^{HF}_{P^{201}} = -\frac{1}{2} a^{HF}_{P^{201}} - \frac{5}{8} b^{HF}_{P^{201}} \\
\Delta E^{HF}_{F=7/2} &= \frac{a^{HF}_{P^{201}}(6)}{2} + \left(\frac{(+6)(+6+1)-30}{48}\right) b^{HF}_{P^{201}} = 3 a^{HF}_{P^{201}} + \frac{1}{4} b^{HF}_{P^{201}}
\end{aligned}\right\}$$

The splittings between the states (noting the ½ state is also at a larger energy) are then:

$$\left.\begin{aligned}
&\left|\Delta E^{HF}_{F=1/2} - \Delta E^{HF}_{F=3/2}\right| = 5{,}377\ MHz = \left(-\frac{3}{2} a^{HF}_{P^{201}} + \frac{7}{8} b^{HF}_{P^{201}}\right) \\
&\left|\Delta E^{HF}_{F=3/2} - \Delta E^{HF}_{F=5/2}\right| = 8{,}629\ MHz = \left(-\frac{5}{2} a^{HF}_{P^{201}} + \frac{5}{8} b^{HF}_{P^{201}}\right) \\
&\left|\Delta E^{HF}_{F=5/2} - \Delta E^{HF}_{F=7/2}\right| = 11{,}382\ MHz = \left(-\frac{7}{2} a^{HF}_{P^{201}} - \frac{7}{8} b^{HF}_{P^{201}}\right) \\
&\therefore -12 a^{HF}_{P^{201}} + 7 b^{HF}_{P^{201}} = 43{,}016\ MHz; -20 a^{HF}_{P^{201}} + 5 b^{HF}_{P^{201}} = 69{,}032\ MHz \\
&-28 a^{HF}_{P^{201}} - 7 b^{HF}_{P^{201}} = 91{,}056\ MHz \\
&\therefore -60 a^{HF}_{P^{201}} + 35 b^{HF}_{P^{201}} = 215080\ MHz; -140 a^{HF}_{P^{201}} + 35 b^{HF}_{P^{201}} = 483224\ MHz \\
&\therefore 80 a^{HF}_{P^{201}} = -268144 \Rightarrow a^{HF}_{P^{201}} = -3351.8\ MHz \\
&\therefore -12(-3351.8) + 7 b^{HF}_{P^{201}} = 43{,}016\ MHz \\
&\Rightarrow 7 b^{HF}_{P^{201}} = 2794.4 \Rightarrow b^{HF}_{P^{201}} = +399.2\ MHz \\
&\therefore \Delta E^{HF}_{F=1/2} = -\frac{9}{2} a^{HF}_{P^{201}} + \frac{7}{8} b^{HF}_{P^{201}} = +15{,}432.4\ MHz \\
&\Delta E^{HF}_{F=3/2} = -3 a^{HF}_{P^{201}} = +10{,}055\ MHz \\
&\Delta E^{HF}_{F=5/2} = -\frac{1}{2} a^{HF}_{P^{201}} - \frac{5}{8} b^{HF}_{P^{201}} = +1426.4\ MHz \\
&\Delta E^{HF}_{F=7/2} = 3 a^{HF}_{P^{201}} + \frac{1}{4} b^{HF}_{P^{201}} = -9{,}956\ MHz
\end{aligned}\right\} \qquad \text{(A15)}$$

So in summary we have the following magnetic dipole and electrostatic quadrupole constants for the hyperfine components in MHz (as evaluated from the different values of the splittings taken from the high-resolution laser spectroscopy [Sansonetti et al]). ***Curiously this paper does not calculate these***:

$$
\left.
\begin{array}{l}
a_{S^{201}}^{HF} = -7{,}947.83\ \text{MHz}; b_{S^{201}}^{HF} = +2.02\ \text{MHz} \\
a_{S^{201}}^{HF} = -7{,}946.66\ \text{MHz}; b_{S^{201}}^{HF} = +2.80\ \text{MHz} \\
a_{S^{201}}^{HF} = -7{,}946.00\ \text{MHz}; b_{S^{201}}^{HF} = +9.33\ \text{MHz}
\end{array}
\right\} \Rightarrow \left\langle a_{S^{201}}^{HF} \right\rangle = -7{,}946.66\ \text{MHz}; \left\langle b_{S^{201}}^{HF} \right\rangle = +4.72\ \text{MHz}
\tag{A16}
$$

$$
a_{S^{199}}^{HF} = +21{,}500\ \text{MHz}
$$

$$
a_{P^{199}}^{HF} = +9{,}066.4\ \text{MHz}
$$

$$
a_{P^{201}}^{HF} = -3351.8\ \text{MHz}; b_{P^{201}}^{HF} = +399.2\ \text{MHz}
$$

Demonstrator Exercise A1. From equations A2 and A5 show that the hyperfine energy level diagram is as given in Figure A2.

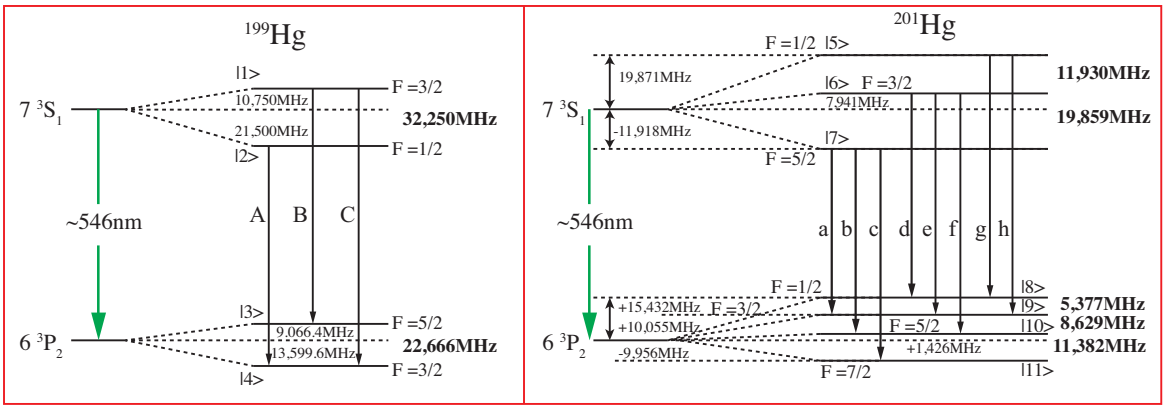

FIG A2. Hyperfine energy levels in ^{199}Hg & ^{201}Hg, with relative separations calculated from the HFS Hamiltonian with respect to the fine structure states. The 11 dipole allowed transitions (A-C) and (a-h) are also shown (see text for details).

Dipole Allowed Transitions.

Radiation from the upper state to the lower state can only occur if the angular momentum of the system (atom + photon) is conserved. Since photons carry angular momentum, this leads to the following dipole allowed selection rules for the hyperfine state transitions:

$$\Delta \boldsymbol{F} = \pm 1, 0 \qquad \text{(A17)}$$

This leads to 3 possible transitions for the ^{199}Hg isotope and 8 possible transitions for the ^{201}Hg isotope, as is shown in Figure A2.

The table below gives the experimentally measured spacing's between isotopes for the mass shifts as well as a link to the hyperfine state transitions, referenced to the ^{198}Hg line.

Hg Isotope	Frequency shift (MHz)	Abundance
^{196}Hg	Not observed	0.15%
^{198}Hg	0 MHz (reference line)	9.97%
^{199}Hg transition A from |2> to |4>	-7776.212MHz	16.87%
^{200}Hg	+846.445MHz	23.1%
^{201}Hg transition c from |7> to |11>	-831.578MHz	13.2%
^{202}Hg	+1775.645MHz	29.9%
^{204}Hg	+2689.972MHz	6.87%

Table A1. The Hg isotopes and frequency positions from the ^{198}Hg transition and their relative abundances.

Demonstrator Exercise A2. You should calculate the possible transition frequencies from the data in figure A2 as well as that given in Table A1. It is these frequencies that will be compared to the experimental results.

Establishing the values of a and b from the experimental data.

The Fabry Perot etalon has a free spectral range of 37,500 MHz and a finesse of 43, so the Doppler free peaks in the spectrum will have a repeat pattern over this range. Since the range of the hyperfine structure is from around -21,000 MHz to +24500 MHz, the spectrum cannot be contained within 1 FSR range and so will wrap around as shown in the figure below, which represents 3 orders of the Fabry Perot in frequency space. This spectrum is reproduced from [Sansonetti et al]. Each peak will be broadened by the Airy function of the etalon, as well as due to the natural linewidth of the transition, collisional broadening and Doppler broadening in the lamp. A convolution over each of these effects hence needs to be carried out to establish how the signal from the lamp is produced on the camera. *Note that the intensities of the lines may not be the same for the laser excitation process compared to that from the etalon due to polarization of the laser and optical pumping, so this is only a guide wrt intensity.*

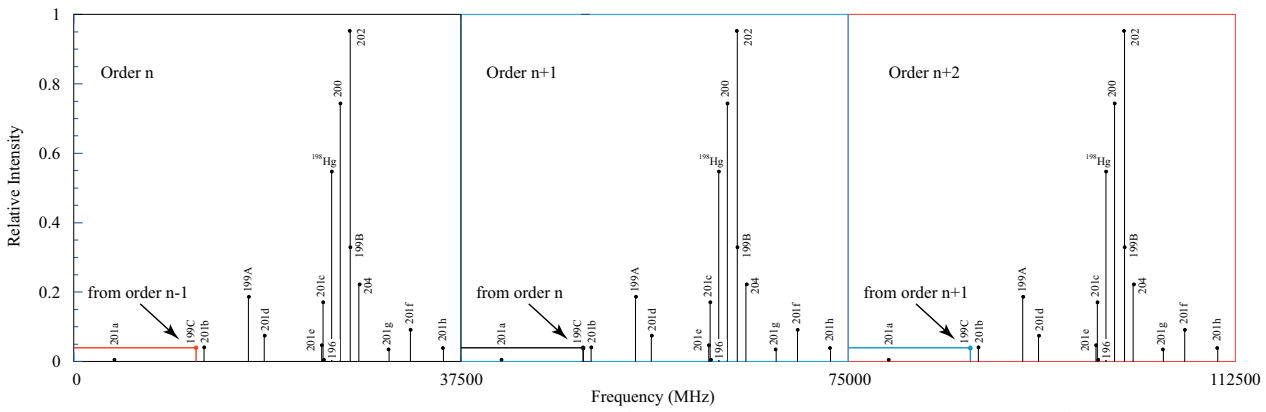

Authors: Rosie Barnes, Edward Wilson and Andrew James Murray

FIG A3. Doppler free signal showing how the spectrum wraps around due to the 37.5 GHz FSR of the etalon, repeated for 3 orders. The frequency spacing for an etalon is linear as shown.

Note that due to the 37.5 GHz free spectral range the 199C line will appear to 'wrap around' and so the peak will be found at a position close to the 201b line. The 199C peak is hence from the *previous* order in the etalon signal as shown. The absolute value of the order cannot be distinguished using an etalon.

The actual experimental data from the Fabry Perot interferometer yields far less precise values of the peaks compared to the laser experiments, as shown below. The list shows their positions where peak G was used as a reference in the experimental fits and all other peak positions were measured with respect to this reference. The frequencies are also shown using peak E as a reference since it is the leftmost peak in the etalon spectrum shown. The transitions that give rise to the different peaks are given in table 2, based upon the information from the fits as in figure A4.

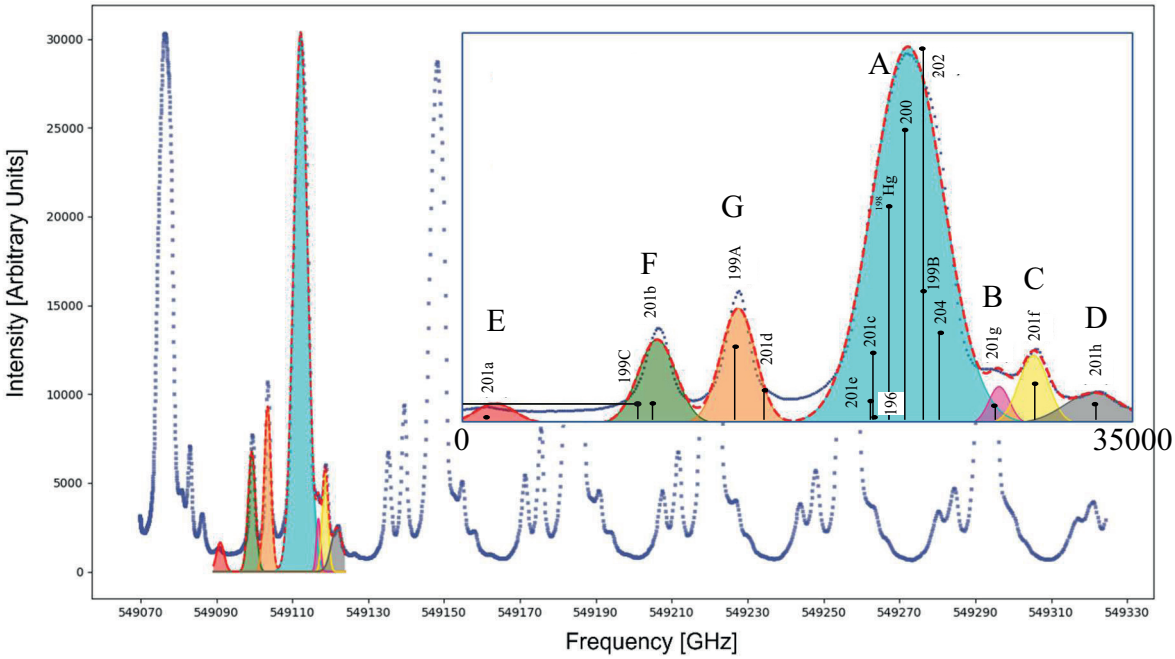

FIG A4. Signal from the etalon compared to the Doppler free positions of the peaks in figure 2. The inset shows the fits to the data over a 35GHz range.

FP Line	Laser Line	Transition	Relative Frequency from G	Relative Frequency from E	Laser Frequency from E
A1	196-204	Even Isotopes $\left({}^{196}\text{Hg} - {}^{204}\text{Hg}\right)$	+8660 MHz ± 1090 MHz	+21740 MHz ± 1090 MHz	20093.5-23533.7 MHz
A2	201e	${}^{201}\text{Hg}\ 7^3S_1(F=3/2)$ to $6^3P_2(F=3/2)$	+8660 MHz ± 1090 MHz	+21740 MHz ± 1090 MHz	19866.94 MHz
A3	201c	${}^{201}\text{Hg}\ 7^3S_1(F=5/2)$ to $6^3P_2(F=7/2)$	+8660 MHz ± 1090 MHz	+21740 MHz ± 1090 MHz	20012.15 MHz
A4	199B	${}^{199}\text{Hg}\ 7^3S_1(F=3/2)$ to $6^3P_2(F=5/2)$	+8660 MHz ± 1090 MHz	+21740 MHz ± 1090 MHz	22664.23 MHz
B	201g	${}^{201}\text{Hg}\ 7^3S_1(F=1/2)$ to $6^3P_2(F=1/2)$	+13380 MHz ± 1280 MHz	+26460 MHz ± 1280 MHz	26415.92 MHz
C	201f	${}^{201}\text{Hg}\ 7^3S_1(F=3/2)$ to $6^3P_2(F=5/2)$	+14980 MHz ± 1090 MHz	+28060 MHz ± 1090 MHz	28496.46 MHz
D	201h	${}^{201}\text{Hg}\ 7^3S_1(F=1/2)$ to $6^3P_2(F=3/2)$	+18240 MHz ± 1430 MHz	+31320 MHz ± 1430 MHz	31793.42 MHz
E	201a	${}^{201}\text{Hg}\ 7^3S_1(F=5/2)$ to $6^3P_2(F=3/2)$	-13080 MHz ± 3980 MHz	0 MHz ± 3980 MHz	0 MHz
F1	199C	${}^{199}\text{Hg}\ 7^3S_1(F=3/2)$ to $6^3P_2(F=3/2)$	- 4300 MHz ± 1430 MHz	+8780 MHz ± 1430 MHz	7817.63(45317.63) MHz
F2	201b	${}^{201}\text{Hg}\ 7^3S_1(F=5/2)$ to $6^3P_2(F=5/2)$	- 4300 MHz ± 1430 MHz	+8780 MHz ± 1430 MHz	8629.52 MHz
G1	199A	${}^{199}\text{Hg}\ 7^3S_1(F=1/2)$ to $6^3P_2(F=3/2)$	0 MHz ± 970 MHz	+13080 MHz ± 970 MHz	13067.52 MHz
G2	201d	${}^{201}\text{Hg}\ 7^3S_1(F=3/2)$ to $6^3P_2(F=1/2)$	0 MHz ± 970 MHz	+13080 MHz ± 970 MHz	14489.45 MHz

Table 2. Peak positions and uncertainties fitted to the experimental data in figure A4, together with their assigned peaks from the Doppler free laser spectrum. The red F1 line is a wrap around signal from the previous order as

explained above. The results from the accurate laser measurements are also shown for reference. The lines A1 – A4, F1 – F2 and G1 – G2 cannot be resolved in the experiment and so only their peak value can be used here.

To calculate the a & b coefficients from the actual experimental data we need to know the frequency differences between the states as shown in Fig A2, reproduced here in figure A5 to demonstrated this.

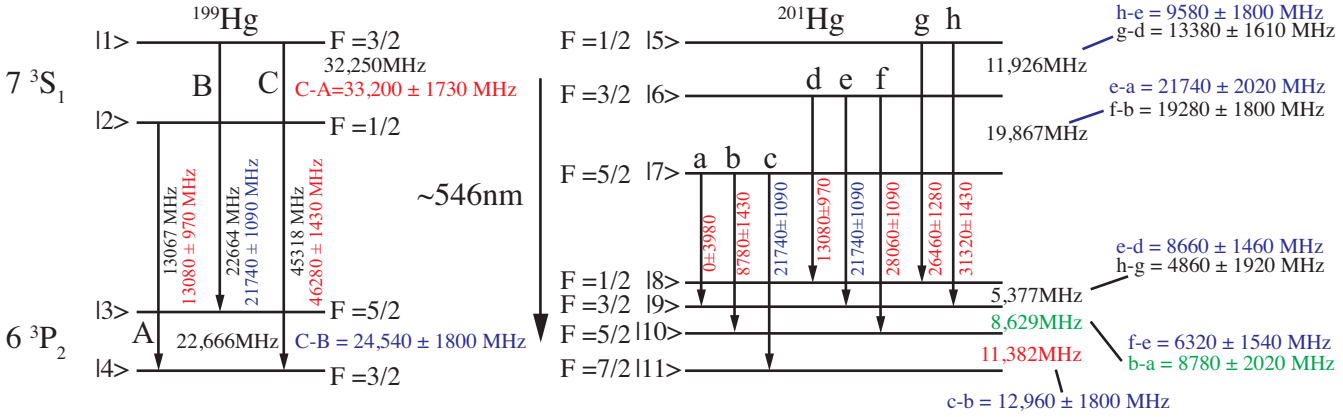

FIG A5. Calculated frequency differences from the etalon signals. The frequencies in blue are from the large central peak and so are only used if no other transitions are available, since these have a large uncertainty due to not knowing where in the peak the state transition arises.

The frequency shifts from the experiment are hence given by:

$$
\begin{aligned}
&{}^{199}Hg7^3S_1 = 33{,}200 \pm 1730\,MHz \\
&{}^{199}Hg6^3P_2 = 24{,}540 \pm 1800\,MHz
\end{aligned}
$$

$$
\begin{aligned}
&{}^{201}Hg7^3S_1\left(F = 1/2 - F = 3/2\right) = 13{,}380 \pm 1610\,MHz \\
&{}^{201}Hg7^3S_1\left(F = 3/2 - F = 5/2\right) = 19{,}280 \pm 1800\,MHz \\
&{}^{201}Hg6^3P_2\left(F = 1/2 - F = 3/2\right) = 4{,}860 \pm 1920\,MHz \\
&{}^{201}Hg6^3P_2\left(F = 3/2 - F = 5/2\right) = 8{,}780 \pm 2020\,MHz \\
&{}^{201}Hg6^3P_2\left(F = 5/2 - F = 7/2\right) = 12{,}960 \pm 1800\,MHz
\end{aligned}
\qquad \text{(A18)}
$$

From these we can calculate the relative a & b coefficients as shown below.

From the equations above we have:

$$
\begin{aligned}
&{}^{199}Hg7^3S_1 = 33{,}200 \pm 1730\,MHz \\
&\Rightarrow \frac{3}{2}a^{HF}_{S^{199}} = 33{,}200 \pm 1730\,MHz \Rightarrow a^{HF}_{S^{199}} = 22{,}133 \pm 1160\ \text{MHz} \\
&\text{Actual } a^{HF}_{S^{199}} = 21{,}500\ \text{MHz} \\
&{}^{199}Hg6^3P_2 = 24{,}540 \pm 1800\,MHz \\
&\Rightarrow \frac{5}{2}a^{HF}_{S^{199}} = 24{,}540 \pm 1800\ \text{MHz} \Rightarrow a^{HF}_{P^{199}} = 9{,}816 \pm 720\ \text{MHz} \\
&\text{Accurate } a^{HF}_{P^{199}} = 9{,}066.4\ \text{MHz}
\end{aligned}
\qquad \text{(A19)}
$$

So the experimental results for the ^{199}Hg states agree with the accurate calculation, to within $\pm 1\sigma$.

From above we have:

$$
\begin{aligned}
&{}^{201}Hg7^3S_1\left(F=1/2-F=3/2\right)=13{,}380\pm1610\,MHz\\
&{}^{201}Hg7^3S_1\left(F=3/2-F=5/2\right)=19{,}280\pm1800\,MHz\\
&\left|\Delta E^{HF}_{F=1/2}-\Delta E^{HF}_{F=3/2}\right|=13{,}380\pm1610\,MHz=\left(-\frac{3}{2}a^{HF}_{S^{201}}+\frac{9}{4}b^{HF}_{S^{201}}\right)\\
&\left|\Delta E^{HF}_{F=3/2}-\Delta E^{HF}_{F=5/2}\right|=19{,}280\pm1800\,MHz=\left(-\frac{5}{2}a^{HF}_{S^{201}}-\frac{5}{4}b^{HF}_{S^{201}}\right)\\
&\left|\Delta E^{HF}_{F=1/2}-\Delta E^{HF}_{F=5/2}\right|=32{,}660\pm2420\,MHz=\left(-4a^{HF}_{S^{201}}+b^{HF}_{S^{201}}\right)\\
&\Rightarrow\left\langle a^{HF}_{S^{201}}\right\rangle=\text{-}7683.24\pm740\,MHz;\left\langle b^{HF}_{S^{201}}\right\rangle=+1496\pm1600\,MHz
\end{aligned}
\qquad\text{(A20)}
$$

$$
\text{Accurate}\left\langle a^{HF}_{S^{201}}\right\rangle=-7{,}946.71\,MHz;\left\langle b^{HF}_{S^{201}}\right\rangle=+4.79\,MHz
$$

So the experimental results for the ^{201}Hg S-state agrees with the accurate calculation, to within $\pm1\sigma$. However the value of the quadrupole constant has a very large error. From equation (15) we also have:

$$
\begin{aligned}
&{}^{201}Hg6^3P_2\left(F=1/2-F=3/2\right)=4{,}860\pm1920\,MHz\\
&{}^{201}Hg6^3P_2\left(F=3/2-F=5/2\right)=8{,}780\pm2020\,MHz\\
&{}^{201}Hg6^3P_2\left(F=5/2-F=7/2\right)=12{,}960\pm1800\,MHz\\
&\therefore\left|\Delta E^{HF}_{F=1/2}-\Delta E^{HF}_{F=3/2}\right|=4{,}860\pm1920\,MHz=\left(-\frac{3}{2}a^{HF}_{P^{201}}+\frac{7}{8}b^{HF}_{P^{201}}\right)\\
&\left|\Delta E^{HF}_{F=3/2}-\Delta E^{HF}_{F=5/2}\right|=8{,}780\pm2020\,MHz=\left(-\frac{5}{2}a^{HF}_{P^{201}}+\frac{5}{8}b^{HF}_{P^{201}}\right)\\
&\left|\Delta E^{HF}_{F=5/2}-\Delta E^{HF}_{F=7/2}\right|=12{,}960\pm1800\,MHz=\left(-\frac{7}{2}a^{HF}_{P^{201}}-\frac{7}{8}b^{HF}_{P^{201}}\right)\\
&\therefore\left\langle a^{HF}_{P^{201}}\right\rangle=\text{-}3629.14\pm668\,\text{MHz};\left\langle b^{HF}_{P^{201}}\right\rangle=\text{-}584.4\pm1893\,\text{MHz}\\
&\text{Accurate }\ a^{HF}_{P^{201}}=-3351.8\text{ MHz};b^{HF}_{P^{201}}=+399.2\text{ MHz}
\end{aligned}
\qquad\text{(A21)}
$$

So the experimental results for the ^{201}Hg P-state agrees with the accurate calculation, to within $\pm1\sigma$. However the value of the quadrupole constant again has a very large error.

The table below summarises the results from the etalon as well as from the laser experiments

State	Accurate a value	Accurate b value	Experimental a value	Exprimental b value
^{199}Hg 7^3S_1	+21,500 MHz	N/A	+22,133±1160 MHz	N/A
^{199}Hg 6^3P_2	+9,066.4 MHz	N/A	+9,816±720 MHz	N/A
^{201}Hg 7^3S_1	-7,946.66 MHz	+4.72 MHz	-7,683.24±740 MHz	+1,496±1,600 MHz
^{201}Hg 6^3P_2	-3,351.8 MHz	+399.2 MHz	-3,629.14±668 MHz	-584.4±1,893 MHz

Table 3. Results from analysis of the data for calculating the dipole and quadrupole constants for the hyperfine transitions in mercury.

Deriving The Fabry Perot etalon equations.

An etalon is constructed from either solid material (eg fused silica) or may be constructed from mirrors. Consider simplest case where etalon is constructed with an air gap between mirrored surfaces.

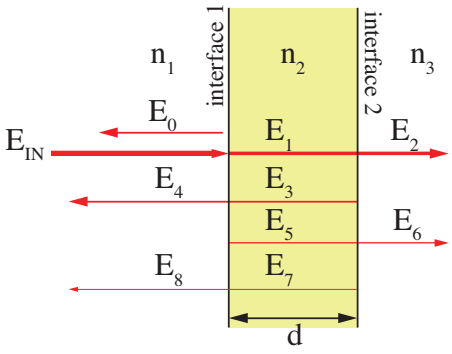

Hence $n_1 = n_3 > 1; n_2 = 1 < n_1$ so phase shift of 0° on reflection of E_{IN} to form E_0.

E_1 passes to interface 2 where it is transmitted (E_2) with 0° phase shift & reflected (E_3) with 180° phase shift since $n_2 < n_3$. E_3 then transmitted (E_4) with 0° phase shift & reflected (E_5)with 180° phase shift at interface 1 and so on.

Let intensity reflection and transmission coefficients at interfaces be given by:

$$\underbrace{r_1, t_1}_{interface1} \; ; \; \underbrace{r_2, t_2}_{interface2}$$

For an air-gapped etalon of thickness d = t, phase shifts occur as the beam propagates around the etalon. At the second interface the phase shift given by:

$$\Phi = \frac{2\pi n_2 t}{\lambda} = \frac{2\pi \nu t}{c}$$

Hence have following conditions for the complex amplitudes of the wavefronts:

$$E_0^{z=0} = E_{IN}^{z=0} e^{j0} \sqrt{r_1} = +E_{IN}^{z=0} \sqrt{r_1}$$
$$E_1^{z=0} = E_{IN}^{z=0} \sqrt{t_1} \Rightarrow E_1^{z=d} = E_{IN}^{z=0} e^{j\Phi} \sqrt{t_1}$$
$$\therefore E_2^{z=d} = E_1^{z=d} \sqrt{t_2} = E_{IN}^{z=0} e^{j\Phi} \sqrt{t_1 t_2}$$
$$\therefore E_3^{z=0} = E_3^{z=d} e^{j\Phi} = \left(E_1^{z=d} e^{j\pi}\right) \sqrt{r_2} = -E_1^{z=0} e^{j2\Phi} \sqrt{r_2} = -E_{IN}^{z=0} e^{j2\Phi} \sqrt{t_1 r_2}$$
$$\therefore E_4^{z=0} = E_3^{z=0} \sqrt{t_1} = -E_{IN}^{z=0} e^{j2\Phi} \sqrt{t_1} \sqrt{t_1 r_2}$$
$$\therefore E_5^{z=0} = \left(E_3^{z=0} e^{j\pi}\right) \sqrt{r_1} = +E_{IN}^{z=0} e^{j2\Phi} \sqrt{t_1 r_1 r_2} \Rightarrow E_5^{z=d} = E_{IN}^{z=0} e^{j3\Phi} \sqrt{t_1 r_1 r_2}$$
$$\therefore E_6^{z=d} = E_5^{z=d} \sqrt{t_2} = E_{IN}^{z=0} e^{j3\Phi} \sqrt{t_1 t_2 r_1 r_2}$$
$$\therefore E_7^{z=0} = -E_{IN}^{z=0} e^{j4\Phi} \sqrt{r_2 t_1 r_1 r_2} \Rightarrow E_8^{z=0} = -E_{IN}^{z=0} e^{j4\Phi} \sqrt{t_1 r_2 r_1 r_2 t_1}$$

Hence the field amplitudes for radiation passing through the etalon is given by:

$$E_2^{z=d} = E_{2+4\cdot 0}^{z=d} = E_{IN}^{z=0}\sqrt{t_1}e^{j\Phi}\sqrt{t_2} = E_{IN}^{z=0}\sqrt{t_1 t_2}e^{j\Phi}$$

$$E_6^{z=d} = E_{2+4\cdot 1}^{z=d} = E_{IN}^{z=0}\sqrt{t_1 t_2}e^{j3\Phi}\sqrt{r_1 r_2}$$

$$E_{10}^{z=d} = E_{2+4\cdot 2}^{z=d} = E_{IN}^{z=0}\sqrt{t_1 t_2}e^{j5\Phi}\left(\sqrt{r_1 r_2}\right)^2$$

$$\Rightarrow E_{2+4n}^{z=d} = E_{IN}^{z=0}\sqrt{t_1 t_2}e^{j(2n+1)\Phi}\left(\sqrt{r_1 r_2}\right)^n$$

$$\Rightarrow E_{2+4n}^{z=d} = E_{IN}^{z=0}Te^{j\Phi}e^{j2n\Phi}R^n$$

$$where\ T = \sqrt{t_1 t_2}; R = \sqrt{r_1 r_2}$$

Intensity of radiation transmitted through the etalon is the sum of all amplitudes multiplied by the complex conjugate. Hence:

$$E_{out}^{z=d} = \sum_{n=0}^{\infty} E_{2+4n}^{z=d} = E_{IN}^{z=0}Te^{j\Phi}\sum_{n=0}^{\infty}\left(e^{j2\Phi}R\right)^n = \frac{E_{IN}^{z=0}Te^{j\Phi}}{1-e^{j2\Phi}R}$$

$$\Rightarrow I_{out} = \frac{\varepsilon_0 c}{2}\left(E_{out}^{z=d}\right)\cdot\left(E_{out}^{z=d}\right)^* = \frac{\varepsilon_0 c}{2}\left(E_{IN}^{z=0}\right)^2 T^2\left(\frac{1}{1-e^{j2\Phi}R}\right)\cdot\left(\frac{1}{1-e^{-j2\Phi}R}\right)$$

$$\therefore I_{out} = I_{IN}T^2\frac{1}{\left(1-e^{j2\Phi}R\right)\left(1-e^{-j2\Phi}R\right)} = I_{IN}T^2\frac{1}{1+R^2-R\left(e^{j2\Phi}+e^{-j2\Phi}\right)}$$

$$\therefore I_{out} = I_{IN}\frac{T^2}{\left(1+R^2\right)-2R\cos 2\Phi}$$

From energy conservation (ie assuming no scattering or absorption losses in the etalon) then we have R + T = 1 and so:

$$\frac{I_{out}}{I_{IN}} = \frac{\left(1-R\right)^2}{\left(1+R^2\right)-2R\cos 2\Phi} = \frac{\left(1-R\right)^2}{\left(1+R^2\right)-2R\left(1-2\sin^2\Phi\right)}$$

$$= \frac{\left(1-R\right)^2}{\left(1+R^2-2R\right)+4R\sin^2\Phi} = \frac{\left(1-R\right)^2}{\left(1-R\right)^2+4R\sin^2\Phi} = \frac{1}{1+F_R\sin^2\Phi}$$

$$where\ F_R = \frac{4R}{\left(1-R\right)^2}$$

Define finesse of etalon as

$$F = \frac{\pi\sqrt{F_R}}{2} = \frac{\pi\sqrt{R}}{1-R}$$

This measures the ratio of free spectral range to half width of the frequency bandwidth. For radiation incident on etalon at angle θ we replace the phase shift by:

$$\Phi = \frac{2\pi n_2 t}{\lambda}\cos\theta = \frac{2\pi\nu t}{c}\cos\theta$$

so that:

$$\frac{I_{out}}{I_{IN}} = \frac{1}{1+F_R\sin^2\Phi} = \frac{1}{1+\frac{4R}{\left(1-R\right)^2}\sin^2\left(\frac{2\pi\nu t}{c}\cos\theta\right)} = \frac{1}{1+\frac{4R}{\left(1-R\right)^2}\sin^2\left(\frac{2\pi t}{\lambda}\cos\theta\right)}$$

This is the *Airy function*. Note that peaks occur when this is a maximum, so that the denominator is a minimum. This happens when

$$\sin^2\left(\frac{2\pi t}{\lambda}\cos\theta\right) = 0 \Rightarrow \frac{2\pi t}{\lambda}\cos\theta = n\pi$$

$$\therefore 2t\cos\theta = n\lambda$$

where n is an integer.

Appendix A2. Using the Hg Green Line Apparatus

Two measurements are needed to generate one set of data: the actual signal, and the background. The measurement of the actual signal is done by taking a single 16-bit resolution image of the circular fringe pattern. The measurement of the background is done by taking a second 16-bit image with the same settings, Field Of View (FOV) and conditions as the signal image, with the only change being that the aperture in front of the etalon is closed (and thus the fringe pattern is not produced).
The best way to acquire these measurements is to first allow the lamp to warm up once turned on (~30 minutes) and then to take the signal image with the desired settings (the details of which are described in section 1.1.). After a satisfactory signal image has been acquired, close the aperture in front of the etalon and, without adjusting any other hardware or settings, take a second image for the background. You will be taking off the background from the signal to allow for any stray light.

1. Taking Images

1.1. The canon EOS Utility

When connected to the computer via a USB C-to-A cable, the camera may be remotely operated using the program EOS Utility. EOS Utility can be found at *'C:/Hg Green Line/Canon/EOS Utility/EOS Utility.exe'*. Upon opening the software, select the option 'Remote Shooting', which will open the remote-control panel. Click the button reading 'Live View Shoot' to open the view window. Ensure that the option 'Depth-of-field preview' is 'ON'.
***Note*:** It is important to ensure that the camera is focussed at **infinity**, as stated in the lab script (why?). Under 'Focus' on the live view window, click the rightmost arrows pointing toward the infinity symbol in order to correctly focus the camera.
The control panel gives several options for adjusting the shooting settings. The relevant settings are detailed in Fig. A2.1.

A. Shooting mode. Ensure that this is set to 'M' for manual shooting.
B. Exposure time. A longer time with the shutter open will result in a brighter image, but will also amplify background noise.
C. Aperture size. Increasing the F-number will decrease the size of the aperture. It is advised to keep the aperture fully open at first.
D. ISO speed. Similar to exposure time, a higher ISO speed will result in a brighter image, but will amplify background noise.
E. File format. **L** is jpeg, **RAW** is the file format required for data analysis.
F. File location. The camera has no local storage, so images must be stored directly onto the computer. Store image files onto the provided SD card.

FIG A2.1: The EOS Utility control panel.

Images should be recorded in **RAW** file format and stored onto the SD-cards provided using the USB SD-card reader. **RAW** is a 16-bit image format, which most standard monitors cannot display. Images may be saved in both **RAW** and **JPEG** format at the same time, in order for the 8-bit **JPEG** versions to be used in lab books and reports.

1.2. Canon Digital Photo Professional

The software for analysing images reads **TIFF** format images, not **RAW**. A program called Canon Digital Photo Professional can be used to convert the **RAW** images to **TIFF**. Digital Photo Professional is located at *'C:/Hg Green Line/Canon/Digital Photo Professional 4/Dpp4.exe'*.
Open Digital Photo Professional and navigate to the location of the **RAW** images using the sidebar. Double click on the image to open it in a separate window then select File -> Convert and save. Open the drop-down menu next to 'Save as type:' and select 'TIFF 16-bit'. Leave the other settings as their defaults, choose the name and location of the converted image, and click 'Save'. A progress bar will show when the conversion is complete.

The image is now ready to be analysed.

2. Analysis

2.1. Hg Green Line: Image Analysis

The first programme, 'Hg Green Line: Image Analysis', analyses the TIFF images and produces a dataset from which the hyperfine splitting energies can be found. It can be found at '*C:/Hg Green Line/Hg Green Line: Image Analysis.exe'*.

The fringe pattern exhibits circular symmetry: the intensity over any single diameter cross section of the fringe pattern can be analysed to extract the hyperfine splitting energies. 'Hg Green Line: Image Analysis', exploits this circular symmetry to reduce the signal-to-noise ratio of the extracted data by performing a 360° rotation about the centre of the pattern every 1° and then averages the intensity pixel-wise over each ring diameter.

The information below details which parts of the analysis are performed in which section of this program.

2.1. Sections 1 and 2

Two images may be loaded into 'Hg Green Line: Image Analysis'. The first, loaded in section 1, is the 16-bit TIFF image of the fringe pattern. The second, loaded in section 2, should be a dark background TIFF image taken with the same settings as the fringe image, as discussed above. This image is used to give the systematic errors in intensity on each pixel. **Take this background image with the aperture in front of the etalon closed and the lamp still on.**

2.1. Section 3

Section 3 of the programme calculates the centre of the fringe pattern. The software calculates a guess at the centre position based on several parameters, detailed in Table A2.1.

PARAMETER	DESCRIPTION
INTENSITY THRESHOLD	A binary threshold is applied to the image, which assigns binary 1 or 0 to each pixel depending on the supplied intensity threshold. The maximum intensity that may be recorded on a single pixel is 2^16 * 3 channels (red, green, blue) = 196608. An intensity threshold of 50% will therefore assign all pixels with intensity less than 0.5*196608 = 98304 a binary value of 0, and all those above 98304 a binary value of 1. The threshold should be selected such that only the brightest primary fringes are set to be binary 1, while all dimmer fringes are eliminated. A value of 35% is recommended as a starting point.
NUMBER OF FRINGES TO AVERAGE OVER	The programme calculates a guess of the centre position of the fringes, based on calculating the centre of each bright fringe in the threshold image. More fringes should give a more accurate result.
INITIAL GUESS (X, Y)	The user must provide an initial guess at the pixel integer coordinates of the centre of the fringe pattern. A better guess will yield a more accurate result, though the only requirement on this guess is that it is within the central fringe.

Table A2.1: Parameters for the centre calculation.

Once the parameters have been supplied, press the 'Go' button and the program will calculate a best guess of the centre position. The program will output the threshold image with a red cross marking the calculated centre position. If the calculated position is accurate, proceed to Section 4. If not, modify the provided parameters until the calculated position is correct.

2.1. Section 4

Click the button 'Perform Averaging' and the programme will make an average over the full 360° every 1°, as described above. The programme will initially output the averaged data in the spatial domain with intensity plotted against radius (called the 'S-space'). However, as described in the lab script, it is more natural to display the fringe pattern of a Fabry-Perot etalon in the frequency domain ('F-space'). Once the spatial data has been generated, enter the focal length of the lens for the image being analysed and press the 'Convert to F-space' button.

Both the S-space and F-space data may be saved as a .csv file for your records. Once these have been saved, they are in the following formats:

- S-space data will be saved with the following columns in the .csv file: Radius *(mm)*, Δ(Radius) *(mm),* Intensity *(arbitrary units),* Δ(Intensity) *(arbitrary units).*
- F-space data will be saved with the following columns in the .csv file: Relative_frequency *(MHz)*, Δ(Relative frequency) *(MHz)*, Intensity *(arbitrary units)*, Δ(Intensity) *(arbitrary units).*

2.2. Hg Green Line: Gaussian Fitting

The second programme, 'Hg Green Line: Gaussian Fitting', is used to fit multiple Gaussians to the peaks in the data. It can be found at '*C:/Hg Green Line/Hg Green Line: Gaussian Fitting.exe'*.
In order to calculate the hyperfine splitting energies, the peaks are fitted. Gaussian functions are a good approximation of the shape of the peaks (students may want to discuss why with the demonstrator). 'Hg Green Line: Gaussian Fitting' has the functionality to calculate and subtract a baseline and to fit multiple Gaussians to sections of the data.
Before fitting, identify which peaks correspond to which transitions by considering your theoretical calculations of the hyperfine energy shifts. ***Note:*** This is not trivial. Consider which transitions the energy shifts are measured relative to. Also, by considering the FSR of the etalon, determine which peaks are summations of multiple transitions. Again, students will want to discuss this with the demonstrator before embarking on a detailed analysis of the data you have obtained.
The information below details which parts of the analysis are performed in which section of this programme.

2.2. Section 1

Import the frequency-domain data output by Hg Green Line: Image Analysis.

2.2. Section 2

This section optionally allows the fitting and subtraction of a polynomial baseline to the data. This may be helpful if the programme is struggling to fit multiple Gaussians.
The baseline fitting works by selecting all minima in the pattern that occur below the maximum y-value provided, and then fitting those points to the selected polynomial function. Experiment with the various baseline shapes that are possible. When a satisfactory baseline has been found, subtract it from the data.

2.2. Section 3

Select a region-of-interest (ROI) that contains one entire order. In order to fit multiple Gaussians within this ROI, it is necessary to provide initial guesses of the fit parameters. Fill in the estimated parameters for the number of Gaussians to be fitted and press 'Display' to view these. Adjust the initial guesses as needed until they approximate the peaks present in the ROI, then press 'Fit' in the right-hand box to perform the fitting.
Note: The initial guesses do not have to be perfect, especially the FWHM. It is worth attempting a fit with loosely guessed parameters first, then only returning to tweak the guesses if the fitting fails or is unsatisfactory. If the fitting is running into continual problems, you can open the 'Advanced Settings' to set limits on the fit parameters.
Record the fit parameters and their uncertainties and repeat the fitting for as many orders in the dataset as are feasible.
From the fitted centres of the peaks, calculate the frequency shifts of each peak relative to the ^{198}Hg line and compare these values to those calculated theoretically. Students need to think carefully about the uncertainties in their calculations and justify these in their logbook and to you as demonstrator.

Appendix A3. Summary of what is now in the labscript for demonstrators:

1. A summary of the atomic physics & theory is given to students, as this is not covered in second year **This has been added as an appendix, together with exercises for them to do. As a demonstrator you need to ensure they can do these calculations.**
2. We now give students the values of a, b calculated from the laser experiments as given above & ask them to calculate the appropriate energy level splittings from theory, so that they reproduce the figures & spectra. **This is found in the appendix as exercise.**
3. The theory on the way the etalon works also needs to be considered by students, as they do not know how this works. The labscript asks them to calculate the Airy function from the phase shifts in the etalon, so that they know what the rings represent that are detected by the optics & camera. **The full derivation is given above for demonstrators – this is likely to require input from them, as well as reference to the optics text books given in the labscript.**
4. The experiment requires students to take photos of the ring patterns from the etalon. The python software developed by Edward & Rosie allows them to take the RAW image from the camera, convert it to a TIFF image (so there are no losses), then finds the centre of the ring pattern and rotates the image around this point every 1°. A slice of the data is taken along each horizontal axis at each rotation angle and this is accumulated 360 times, to produce a very clear low noise spectrum of the rings in radial space, as is shown in figure A4 above. This is hundreds of times better than was possible using the older technology where film was used. **Full details of how to run the programmes is in Appendix A2 of the labscript.**
5. The software can convert from radial 'r-space' to frequency space (as is shown above). From this the software can select different 37.5GHz sections of the spectrum and then fit multiple Gaussians to the peaks. This allows the peak positions, magnitudes & widths to be determined. **Details of how to do this is in Appendix A2 of the labscript.**
6. The difference in peak positions can then be calculated as was carried out in the example above to establish the a & b coefficients from the experimental data. These can then be compared to the a & b values given to them (see point 2 above), with the appropriate errors calculated to check how well they compare. **This has been added in the final part of the labscript and will require them to think carefully about the date they have obtained. It will probably require input from demonstrators how to do this so you need to be familiar with this. An example is given above.**

References:

Craig J Sansonetti and Damir Veza. "Doppler-free measurement of the 546 nm line of mercury". In: Journal of Physics B: Atomic, Molecular and Optical Physics 43.20 (Oct. 2010), p. 205003.

BH Bransden and CJ Joachain. Physics of atoms and molecules. Pearson Education, England, 2001.

Alan Corney. Atomic and laser spectrocopy. Clarendon press, Oxford, 1977